JOURNAL OF MATERIALS SCIENCE 33 (1998) 2299–2304

Microstructural development in cast alloys based on the β-NiAl–β′-Ni_2AlTi–γ′-Ni_3Al–α-Cr system

W. F. GALE, Z. A. M. ABDO
Materials Research and Education Center, Auburn University, Auburn AL 36849, USA
E-mail: wfgale@eng.auburn.edu

An investigation of microstructural development in three arc-cast Ni–Al–Cr–Ti multiphase alloys derived from the B2 type β-NiAl phase is presented. Detailed microstructural characterization of Ni–25 at % Al–20 at % Cr–15 at % Ti, Ni–26 at % Al–21 at % Cr–11 at % Ti and Ni–25 at % Al–24 at % Cr–15 at % Ti materials by transmission electron microscopy (TEM), is described. Microstructural development is examined in both the as-cast condition and after 140 h homogenization treatments at both 850 and 1100 °C. The formation of a eutectic between an $L2_1$-type β′ phase (Heusler phase, with a nominal composition of Ni_2AlTi) and elemental α-Cr is examined. The precipitation of α within $\beta^{(\prime)}$ and vice versa, in both the inter- and intradendritic regions, is considered. The formation of $L1_2$-type γ′ (nominally Ni_3Al) precipitates within the β and β′-phases is discussed, as is the transformation of β to two-phase β/β′ during ageing. © *1998 Chapman & Hall*

1. Introduction

The production of multiphase microstructures based on the B2-type intermetallic compound NiAl (commonly denoted as the "β" phase) has attracted considerable recent interest (e.g. [1–5]). These multiphase microstructures are intended to enhance either: (a) room-temperature ductility/toughness, or (b) high-temperature creep resistance over that obtainable with single-phase β. Materials based on NiAl–α [4] eutectic systems, where "α" represents a body-centred cubic metal such as chromium or molybdenum, represent an important class of multiphase microstructures intended to enhance room-temperature toughness. Ductility/toughness enhancement by the addition of both ordered $L1_2$-type γ′ (nominally Ni_3Al) and disordered face-centred cubic (e.g. nickel-base) solid-solutions has also attracted considerable attention (e.g. [6–9]). Multiphase microstructures intended to enhance the creep resistance of NiAl, include alloys [10, 11] strengthened by the precipitation of β′ phases ($L2_1$-type Heusler phases, such as Ni_2AlTi).

In this paper, an investigation is presented of microstructural development in Ni–Al–Cr–Ti alloys containing α and γ′ phases (that offer potential for enhanced ductility/toughness) and β′ (with the intention of providing improved creep resistance). Arc-cast materials are investigated in both the as-cast condition and after 140 h homogenization treatments at both 850 and 1100 °C.

2. Experimental procedure

Arc-cast samples of Ni–25 at % Al–20 at % Cr–15 at % Ti, Ni–26 at % Al–21 at % Cr–11 at % Ti and Ni–25 at % Al–24 at % Cr–15 at % Ti were produced in the form of 30 g buttons. These buttons were each inverted and arc-melted six times to promote mixing. Homogenization treatments were conducted in an argon atmosphere at temperatures of 850 and 1100 °C for 140 h, followed by furnace cooling to room temperature. Selection of the materials examined in the present paper was based on earlier studies by the authors (e.g. [12, 13]) of microstructural development in Ni–Al–Cr alloys with β–γ′–α derived microstructures. For the present work, titanium was included with the intention of promoting the formation of the β′ phase.

Transmission electron microscopy (TEM) specimens were prepared from each of the arc-cast alloys in the as-cast condition and after both 850 and 1100 °C homogenization. Ion milling, rather than electropolishing, was employed to manufacture the TEM specimens, as severe problems with differential polishing have been experienced previously by the authors with alloys of this type. Argon-ion milling was conducted using a Gatan DuoMill employing an accelerating voltage of 5 kV with dual guns operated at a current of 500 μA per gun with gun–specimen angles of 13°. The TEM investigations were supplemented by light and scanning electron microscopy (LM and SEM, respectively). SEM and LM studies were conducted on metallographic samples electroetched at 3 V in a solution consisting of 70 vol % distilled water, 10 vol % glycerol, 15 vol % hydrochloric acid and 5 vol % nitric acid. For analytical investigations, SEM work on polished, but unetched samples was also conducted.

TEM investigations utilized a JEOL JEM 2010 instrument operated at 200 kV. Throughout this paper, the following nomenclature is employed: BF and DF indicate bright-field and dark-field micrographs, respectively, ***B*** represents the beam direction for selected-area diffraction (SAD) patterns and ***g*** indicates the reciprocal lattice vector of the operating reflection in DF images. SEM studies employed a JEOL JSM 840 instrument operated at 20 kV. Analytical studies were conducted using energy-dispersive X-ray spectroscopy (EDS) via ultra-thin window (UTW) detectors and Link Systems Isis analysers attached to the JEM 2010 and JSM 840 instruments. Quantitative SEM-based and qualitative TEM-based analyses were performed.

3. Results and discussion

In this section the microstructural features of the Ni–25 at % Al–20 at % Cr–15 at % Ti, Ni–26 at % Al–21 at % Cr–11 at % Ti and Ni–25 at % Al–24 at % Cr–15 at % Ti alloys investigated in this work will be discussed. The microstructures of these materials are summarized in Table I and compositional data are given in Table II.

3.1. Overall as-cast microstructure

The Ni–25 at % Al–20 at % Cr–15 at % Ti and Ni–26 at % Al–21 at % Cr–11 at % Ti alloys both solidified dendritically (Fig. 1), forming dendrite matrices comprised, respectively, of $L2_1$-type β′ and B2 type β. However, occasional intradendritic β′ precipitates were observed in the as-cast Ni–26 at % Al–21 at % Cr–11 at % Ti alloy. In both the Ni–25 at % Al–20 at % Cr–15 at % Ti material and the Ni–26 at % Al–21 at % Cr–11 at % Ti alloy, solidification terminated with the formation of a eutectic. However, the character of the eutectic differed between the Ni–25 at % Al–20 at % Cr–15 at % Ti alloy and Ni–26 at % Al–21 at % Cr–11 at % Ti material, in that a β′–α mixture was produced in the former case (Fig. 2) and a β–α combination in the latter. Furthermore, a β′–α eutectic mixture was observed to comprise the entire as-cast microstructure of the Ni–25 at % Al–24 at % Cr–15 at % Ti alloy.

In all of the materials examined in the present work, the A2 type (i.e. body-centred cubic) α-phase was based on chromium with some nickel in solid solution. The α-phase contained only small amounts of aluminium and titanium. The β–α and β′–α eutectic mixtures were generally lamellar, although regions containing roughly rod-shaped α were also observed. A cube–cube orientation relationship was observed between the $\beta^{(\prime)}$ and α constituents of these eutectic mixtures. However, in some localized regions, a significant misorientation (up to around 5° in some cases) was noted between the $\beta^{(\prime)}$ and α phases.

The β′ and β-phases have nominal compositions of Ni_2AlTi and NiAl, respectively. These compositions were not achieved exactly in the present work: both β and β′ were nickel-enriched and contained a small amount of chromium and the β-phase incorporated

TABLE I Summary of microstructural observations (bal. indicates the balance and eutc the eutectic)

Overall as-cast composition (at %)				As-cast (at %)				Aged 140 h at 850 °C (at %)				Aged 140 h at 1100 °C (at %)			
				Dendritic region		Interdendritic region		Dendritic region		Interdendritic region		Dendritic region		Interdendritic region	
Ni	Al	Cr	Ti	Matrix	Second phases	Matrix	Second phases	Matrix	Second phases	Matrix	Second phases	Matrix	Second phases	Matrix	Second phases
bal.	25	20	15	β′	α	β′–α eutc	None	β′	α	β′–α eutc	α in β′	β′	α	β′–α eutc	None
									γ′				γ′		
bal.	26	21	11	β	β′	β–α eutc	γ′ layer	β	α	β/β′ – α	α + γ′ in β/β′	β	α	α	None
					α				γ′		β in α				
bal.	25	24	15		None	β′–α eutc	None		None	β′–α eutc	α in β′		None	β′–α eutc	None

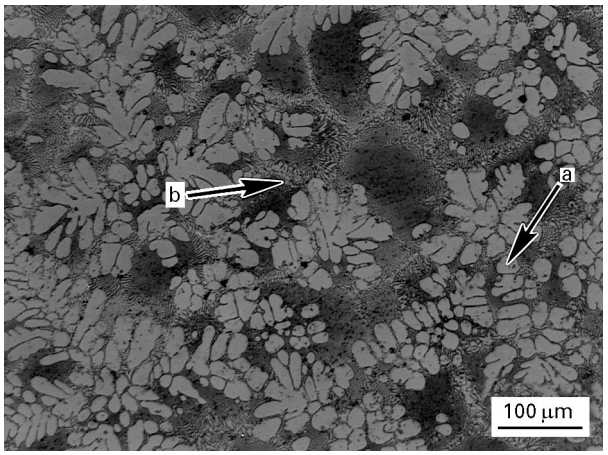

Figure 1 LM image showing the overall microstructure of the Ni–25 at % Al–20 at % Cr–15 at % Ti material (sample aged for 140 h at 850 °C; a, β′ dendrite; b, β′–α eutectic).

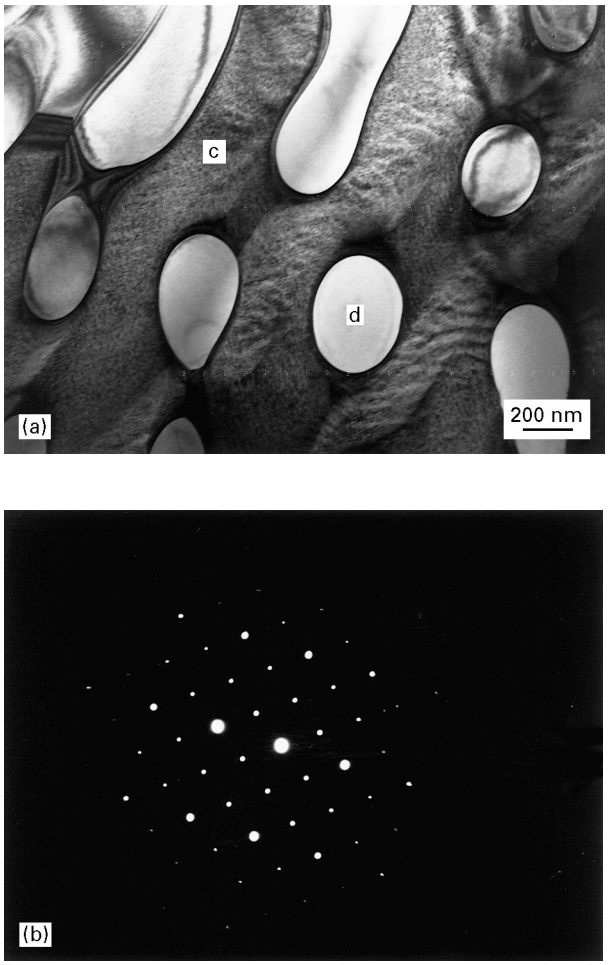

Figure 2 Microstructure of the β′–α eutectic mixture. (a) BF micrograph showing the as-cast Ni–25 at % Al–20 at % Cr–15 at % Ti alloy (c, β′, d, α). (b) SAD pattern with $\boldsymbol{B} = [1\,1\,0]_{\alpha,\beta'}$ showing the cube–cube orientation relationship of the eutectic β′ and α phases (Ni–25 at % Al–24 at % Cr–15 at % Ti alloy aged for 140 h at 850 °C).

some titanium in solid solution. Nonetheless, the formation of β′ dendrites in the titanium-rich Ni–25 at % Al–20 at % Cr–15 at % Ti alloy and β-phase dendrites in the lower-titanium Ni–26 at % Al–21 at % Cr–11 at % Ti material is unsurprising. The presence of a eutectic containing α-Cr in these materials correlates with rejection of chromium back into the liquid by the growing $\beta^{(\prime)}$ phase (as can be seen from the post-solidification EDS data contained in Table II). Furthermore, the formation of a microstructure comprised entirely of a lamellar β′–α eutectic in the Ni–25 at % Al–24 at % Cr–15 at % Ti alloy is not unreasonable, given that this alloy is both titanium- and chromium-rich.

3.2. The influence of ageing on the dendritic and interdendritic matrices

With some notable exceptions, ageing at both 850 and 1100 °C had relatively little effect on the microstructure of either the dendritic or interdendritic matrices of the materials examined. The exceptions to this tendency all occurred in the interdendritic region of the Ni–26 at % Al–21 at % Cr–11 at % Ti material. When aged at 850 °C, the β-phase portion of the β–α eutectic in this alloy decomposed to form a two-phase mixture of β and β′. Thus, the resulting transformed eutectic consisted of β/β′–α (Fig. 3). As has been observed previously in β/β′ alloys (e.g. [10]), the β and β′ were cube–cube orientation related and the interface between these two phases was semicoherent. The β/β′ was, in general, roughly lamellar. However, the lamellar width within the β/β′ region (typically around 100–200 nm) was far smaller than that of the eutectic itself (the α and β′ lamellae constituting the as-cast eutectic typically possessed widths of around a few micrometres, although a wide range of lamellar spacings was observed).

Ageing the Ni–26 at % Al–21 at % Cr–11 at % Ti material at 1100 °C resulted in significant growth of the β-phase dendrites at the expense of the interdendritic region. This process left a rump interdendritic region comprised entirely of single-phase α-Cr. Ageing of this same alloy at 850 °C led to the formation of β-phase precipitates within the eutectic α-phase (Fig. 3). These β-phase precipitates were spheroidal, typically with a diameter of around 10–50 nm. A cube–cube orientation relationship was observed between the β and α phases.

3.3. Precipitation of intradendritic and interdendritic α as a second-phase

In the as-cast condition, α was present as an intradendritic second phase in the two dendrite-forming alloys examined. These α precipitates were cube–cube orientation related to the dendrite matrix (i.e. β or β′). The α-phase formed as spherical precipitates, with a diameter typically in the range of 10–50 nm. The finer precipitates (Fig. 4) in this range formed coherent, elastically strained interfaces with the matrix. In contrast, the coarser precipitates were semicoherent, as has been observed previously for β-phase materials containing α-precipitates (e.g. [14]). Ageing at both 850 and 1100 °C maintained the existing intradendritic α precipitates and initiated some additional intradendritic α deposits.

TABLE II Average dendritic and interdendritic compositions in the as-cast condition and after ageing at 850 and 1100 °C (bal. indicates balance)

Overall as-cast composition (at %)				As-cast (at %)								Aged 140 h at 850 °C (at %)								Aged 140 h at 1100 °C (at %)							
				Average dendritic composition				Average interdendritic composition				Average dendritic composition				Average interdendritic composition				Average dendritic composition				Average interdendritic composition			
Ni	Al	Cr	Ti	Ni	Al	Cr	Ti	Ni	Al	Cr	Ti	Ni	Al	Cr	Ti	Ni	Al	Cr	Ti	Ni	Al	Cr	Ti	Ni	Al	Cr	Ti
bal.	25	20	15	bal.	28	6	19	bal.	22	28	14	bal.	29	9	17	bal.	23	26	13	bal.	27	8	18	bal.	5	75	7
bal.	26	21	11	bal.	28	11	11	bal.	12	63	5	bal.	33	10	9	bal.	9	20	14	bal.	29	5	12	bal.	4	78	4
bal.	25	24	15	–	–	–	–	bal.	25	24	15	–	–	–	–	bal.	26	22	16	–	–	–	–	bal.	24	28	15

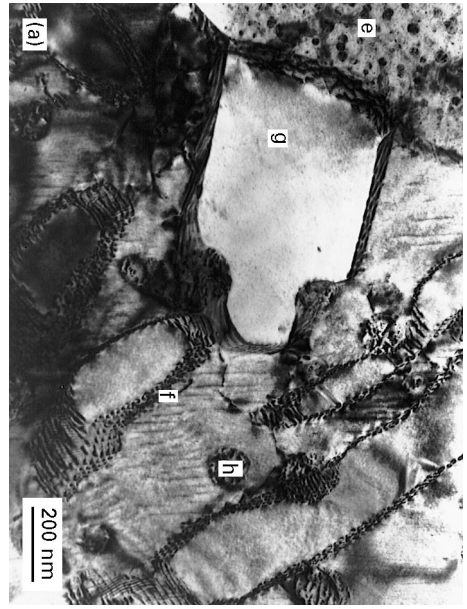

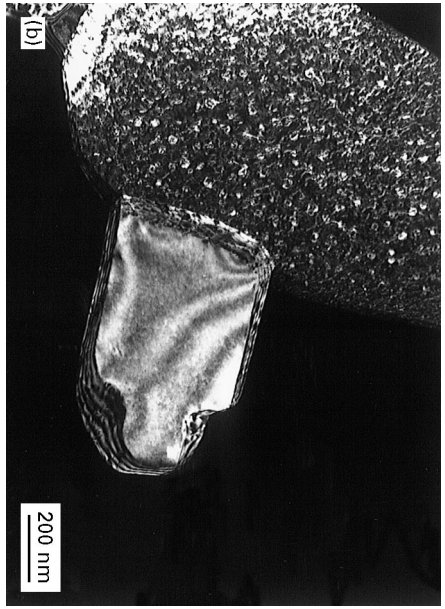

Figure 3 Modification of the interdendritic regions of the Ni–26 at % Al–21 at % Cr–11 at % Ti material as a result of ageing at 850 °C for 140 h. (a) BF micrograph showing the precipitation of β within the eutectic α-phase (e) and the formation of two-phase β/β′ (f) from the eutectic β-phase. The precipitation of γ' (g) on the β/β′–α boundary and α (b) within the β/β′ region are also apparent. (b) DF micrograph of the region shown in (a). This image was recorded using the $\boldsymbol{g} = (1\,1\,1)_{\gamma'}, (1\,1\,0)_{\alpha}$ common reflection. The γ' precipitate is almost exactly cube–cube with the eutectic α, whereas misorientation between the α and β/β′ results in the latter being out of contrast.

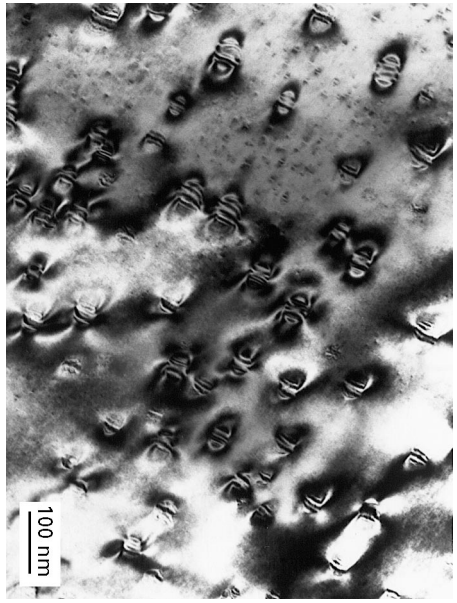

Figure 4 Intradendritic precipitation of α-Cr in the as-cast condition. BF micrograph showing α-Cr precipitates with an elastically strained coherent interface to the β′-phase dendrite matrix of the Ni–25 at % Al–20 at % Cr–15 at % Ti alloy.

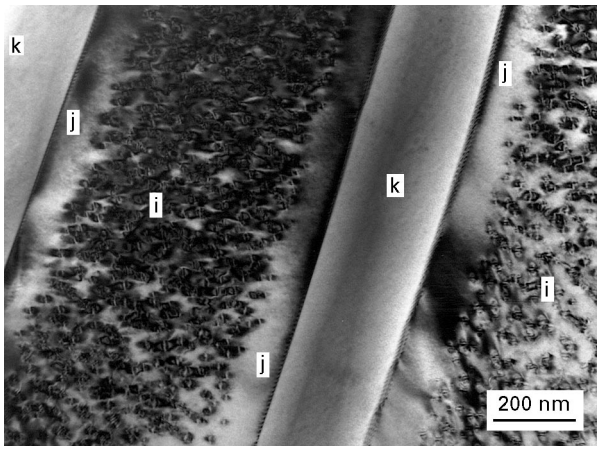

Figure 5 BF image showing the formation of α-Cr within the eutectic β′ phase (i) of the Ni–25 at % Al–20 at % Cr–15 at % Ti alloy aged for 140 h at 850 °C. Note the presence of α precipitate-free zones (j) adjacent to the eutectic α-phase (k).

Ageing at 850 °C complicated the microstructure of the $\beta^{(\prime)}$–α eutectic mixtures of the materials examined. In all cases, α was observed to precipitate (with either a spheroidal or rod-shaped morphology) within the β or β′ portion of the eutectic. A cube–cube orientation relationship was observed between the $\beta^{(\prime)}$ and the α phases. In general, α precipitates were formed throughout the β′ portion of the eutectic. However, in the Ni–25 at % Al–20 at % Cr–15 at % Ti alloy, chromium-depleted regions were observed adjacent to the existing eutectic α-Cr due to growth of these deposits during ageing. These chromium-depleted regions correlated with the formation of precipitate-free zones around the α lamellae (Fig. 5).

3.4. Precipitation of γ′ second phases

The Ni–26 at % Al–21 at % Cr–11 at % Ti material was observed to possess a fringe of interdendritic γ′ needles surrounding the dendrites in the as-cast condition. In contrast, in the as-cast condition, the other two materials examined were free of γ′. The Ni–26 at % Al–21 at % Cr–11 at % Ti material contained numerous interdendritic γ′ precipitates (within the β/β′ regions) after ageing at 850 °C. The two dendritic alloys (Ni–25 at % Al–20 at % Cr–15 at % Ti and Ni–26 at % Al–21 at % Cr–11 at % Ti) also showed extensive intradendritic precipitation of γ′ after ageing (Fig. 6). Both needle-like and ellipsoidal γ′ morphologies were observed within the β or β′ phase. A range of γ′ precipitate sizes was observed with precipitate lengths typically in the range of 500 nm to 1 μm and widths of 50–250 nm. The γ′ precipitates were generally twinned and contained either extensive microtwinning or a single central twinned midrib (twinning in such γ′ precipitates has been discussed elsewhere, e.g. [10, 15, 16]).

In the case of both the intra- and interdendritic precipitation of γ′, orientation relationships of either the Kurdjumov–Sachs

$$[1\,\bar{1}\,1]_{\beta} \parallel [0\,\bar{1}\,1]_{\gamma'}$$

$$(1\,1\,0)_{\beta} \parallel (1\,1\,1)_{\gamma'}$$

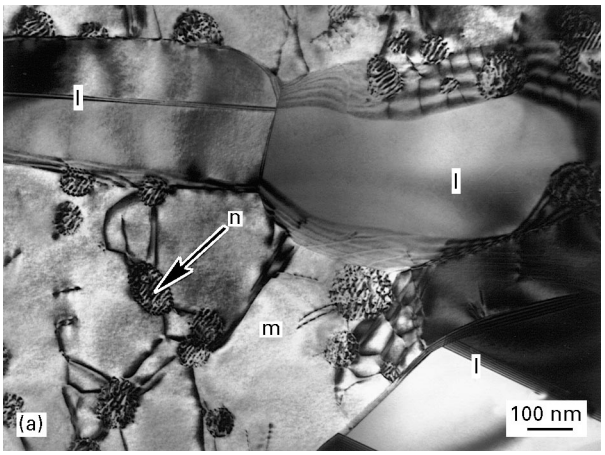

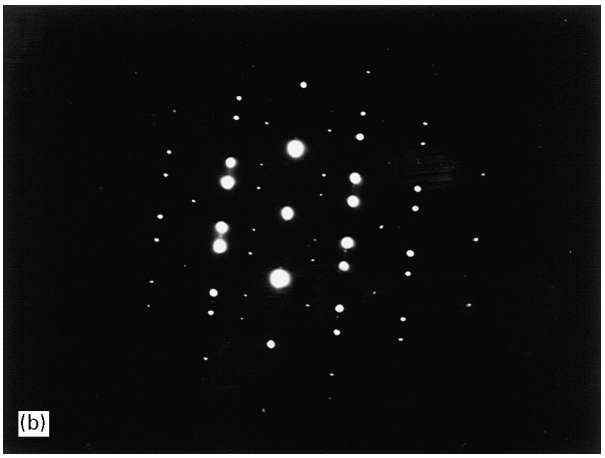

Figure 6 The intradendritic precipitation of twinned γ′ in the Ni–25 at % Al–20 at % Cr–15 at % Ti alloy, aged for 140 h at 850 °C. (a) BF micrograph showing the γ′ precipitates (l) in a β′ matrix (m). The figure also shows α-Cr precipitates (n). (b) SAD pattern with $\boldsymbol{B} = [1\,1\,0]_{\gamma'}$ showing the twinning of a γ′ precipitate.

or Nishiyama–Wasserman (Fig. 7)

$$[0\,0\,1]_{\beta} \parallel [\bar{1}\,0\,1]_{\gamma'}$$

$$(1\,1\,0)_{\beta} \parallel (1\,1\,1)_{\gamma'}$$

type were produced between the γ′ and the surrounding matrix. However, an additional complication was observed in the case of the interdendritic regions. In these regions, a portion of the γ′ (Fig. 3) was nucleated on the $\beta^{(\prime)}$–α boundaries and then grew into the $\beta^{(\prime)}$. In locations where the $\beta^{(\prime)}$ and α phases were significantly misoriented, an exact orientation relationship was invariably established with the α rather than the $\beta^{(\prime)}$.

In summary, amongst the materials investigated, the formation of interdendritic regions containing a $\beta^{(\prime)}$–α eutectic is encouraging from the standpoint of potential for toughening. However, further work will be required to modify the composition and processing of these materials in order to encourage the formation of creep-resisting two-phase β/β′ (rather than either single-phase β or β′ which were generally observed in the present work) both intra- and interdendritically.

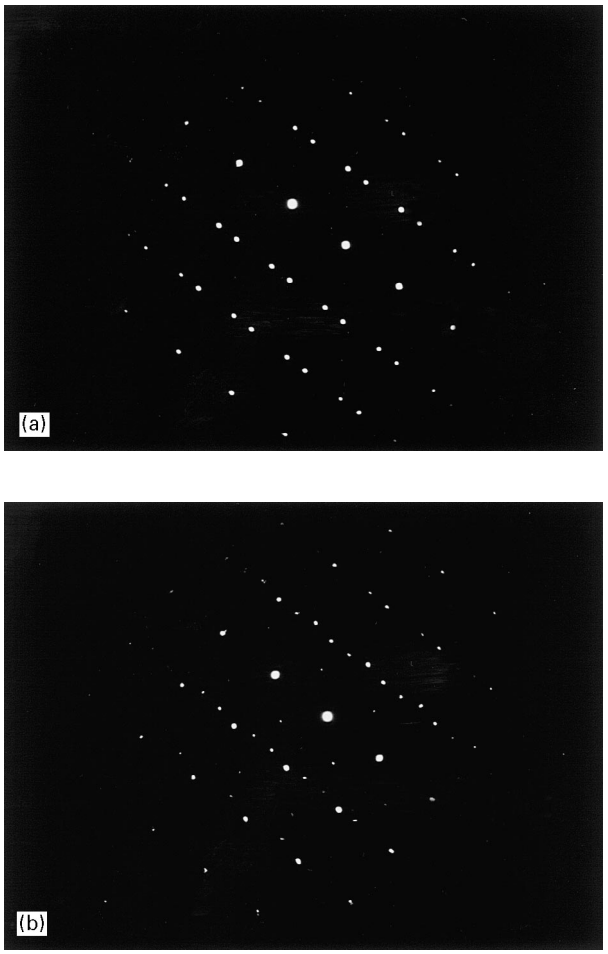

Figure 7 SAD patterns illustrating the formation of a Nishiyama–Wasserman type orientation relationship between the γ' and β-phases in the intradendritic region of the Ni–26 at % Al–21 at % Cr–11 at % Ti material held for 140 h at 850 °C. (a) $\boldsymbol{B} = [\bar{1}\,0\,1]_{\gamma'}$, (b) $\boldsymbol{B} = [0\,0\,1]_{\beta} \parallel [\bar{1}\,0\,1]_{\gamma'}$.

4. Conclusions

A microstructural study of three cast multiphase NiAl-derived alloys, Ni–25 at % Al–20 at % Cr–15 at % Ti, Ni–26 at % Al–21 at % Cr–11 at % Ti and Ni–25 at % Al–24 at % Cr–15 at % Ti has been undertaken. Although the three alloys lay within only a limited range of composition, significant differences were observed between the microstructures of these materials. As a result of this investigation, the following specific conclusions have been drawn.

1. The relatively high titanium content of the Ni–25 at % Al–20 at % Cr–15 at % Ti alloy, when compared with the Ni–26 at % Al–21 at % Cr–11 at % Ti material, correlated with dendritic solidification of these materials to β' and β, respectively.

2. All of the materials investigated formed a two-phase eutectic, involving the α phase and either β or β'. Indeed the chromium-rich Ni–25 at % Al–24 at % Cr–15 at % Ti alloy consisted entirely of a β'–α eutectic. In the two dendritic alloys, chromium segregated strongly to the interdendritic regions and this correlated with the formation of the chromium-rich α-phase. A significant amount of intradendritic α precipitation was also noted.

3. In general, ageing at 850 and 1100 °C did not change the basic microstructure of the materials examined. However, in some cases, ageing did induce extensive precipitation of γ' within the intra- and interdendritic $\beta^{(\prime)}$. Ageing also led to the precipitation of α within the eutectic $\beta^{(\prime)}$ and β within the eutectic α. Decomposition of the eutectic β-phase to two-phase β/β' was observed in the Ni–26 at % Al–21 at % Cr–11 at % Ti material aged at 850 °C.

Acknowledgement

The research discussed in this paper was supported by the National Science Foundation's EPSCoR program.

References

1. R. KAINUMA, K. ISHIDA and T. NISHIZAWA, *Metall. Trans.* **23A** (1992) 1147.
2. K. ISHIDA, R. KAINUMA, N. UENO and T. NISHIZAWA, *ibid.* **22A** (1991) 441.
3. R. D. FIELD, D. D. KRUEGER and S. C. HUANG, *MRS Symp. Proc.* **133** (1989) 567.
4. F. E. HEREDIA, M. Y. HE, G. E. LUCAS, A. G. EVANS, H. E. DEVE and D. KONITZER, *Acta Metall. Mater.* **41** (1993) 505.
5. I. JUNG and G. SAUTHOFF, *Z. Metall.* **80** (1989) 484.
6. K. S. KUMAR, S. K. MANNAN and R. K. VISHWANADHAM, *Acta Metall. Mater.* **40** (1992) 1201.
7. R. YANG, J. A. LEAKE and R. W. CAHN, *MRS Symp. Proc.* **288** (1993) 489.
8. A. MISRA, R. D. NOEBE and R. GIBALA, *ibid.* **288** (1993) 483.
9. *Idem.*, *ibid.* **273** (1992) 205.
10. R. YANG, J. A. LEAKE and R. W. CAHN, *J. Mater. Res.* **6** (1991) 343.
11. P. R. STRUTT and B. H. KEAR, *MRS Symp. Proc.* **39** (1984) 279.
12. W. F. GALE, Z. A. M. ABDO and R. V. NEMANI, *J. Mater. Sci.*, submitted.
13. W. F. GALE, R. V. NEMANI and J. A. HORTON, *ibid.* **31** (1996) 1681.
14. R. D. FIELD, D. F. LAHRMAN and R. DAROLIA, *Acta. Metall. Mater.* **39** (1991) 2961.
15. W. F. GALE, *Intermetallics* **4** (1996) 585.
16. R. KAINUMA, *ibid.* **4** (1996) 37.

Received 29 May 1997
and accepted 27 January 1998